MANEUVERS AROUND JUPITER WITH AUTOMATIC CORRECTION OF THE TRAJECTORY CONSIDERING GRAVITATIONAL DISTURBANCES GENERATED BY THE GALILEAN MOONS: IO, EUROPA GANYMEDE AND CALLISTO

Evandro Marconi Rocco
National Institute for Space Research (INPE), Av. dos Astronautas, 1758,
São José dos Campos, Brazil, evandro.rocco@inpe.br

Abstract: *The goal of this study is to evaluate the influence of the gravitational attraction of the Sun, and the Galilean moons, during orbital maneuvers of a spacecraft orbiting Jupiter. Initially ideal thrusters, capable of applying infinite magnitude of the thrust, were used. Thus, impulsive optimal maneuvers were obtained by scanning the solutions of the Two Point Boundary Value Problem (TPBVP) for various values of transfer time in order to select the impulsive maneuver of minimum necessary velocity increment. Then, the selected maneuver was simulated considering a more realistic model of the propulsion system. In fact is not possible to accomplish an impulsive maneuver. Thus, the orbital maneuver must be distributed in a propulsive arc around the position of the impulse given by the solution of the TPBVP. In this arc was used a continuous thrust, limited to the capacity of the thrusters, with automatic correction of the trajectory. However the effect of the propulsive arc is not exactly equivalent to the application of an impulse. The evaluation of the difference between these approaches is extremely relevant in the mission analysis and spacecraft design of the trajectory control system. Therefore, the influence of the capacity of thrusters in the trajectory was evaluated for a more realistic model instead of the ideal case represented by the impulsive approach.*

Keywords: *Astrodynamics, Orbital Maneuvers, Continuous Thrust, Automatic Correction.*

1. Introduction

In a space mission analysis all aspects related to the spacecraft's mission must be studied and analyzed. Regarding to the orbital maneuvers is important to consider all environmental disturbances applied to the trajectory. In this way, this work aims to evaluate the influence of the gravitational attraction of the Sun, Io, Europa, Ganymede and Callisto, during orbital maneuvers of a spacecraft orbiting Jupiter. Another source of disturbance that should be considered is the non-ideality of the thrusters. So, in the simulations some constructive aspects of the propulsion system were considered. Initially ideal thrusters, capable of applying infinite magnitude of the thrust, were used. Thus, impulsive optimal maneuvers were obtained by scanning the solutions of the Two Point Boundary Value Problem (TPBVP) for various values of transfer time, sweeping all the time range allowed to perform the maneuver, in order to select the maneuver of minimum fuel consumption, which represents the orbital maneuver that requires the minimum total velocity increment. Then, the selected maneuver was simulated considering a more realistic model of the propulsion system. In fact is not possible to accomplish an impulsive maneuver because to perform this kind of maneuver it would be necessary an infinite capacity for the thrusters, because the entire velocity change of the spacecraft should occur instantly. Thus, the orbital maneuver must be distributed in a propulsive arc around the position of the impulse given by the solution of the TPBVP. In this arc was used a continuous thrust, limited to the capacity of the thrusters. However the effect of the propulsive arc is not exactly equivalent to the application of an impulse due to the errors in magnitude and direction of applied thrust. The difference

between these approaches produces a deviation in the trajectory. The evaluation of deviation is extremely relevant in the mission analysis and spacecraft design of the trajectory control system. Therefore, the influence of the capacity of thrusters in the trajectory was evaluated for a more realistic model instead of the ideal case represented by the impulsive approach. Nevertheless, to mitigate the effects of the non-ideality of the thrusters was considered an innovative technique of automatic correction of the trajectory, which performs automatically the adjustment of the semi-major axis of the orbits.

Thus, initially the bi-impulsive maneuver, which consists of finding the transfer orbit that connects a point on the initial orbit to another point in the final orbit spending a certain amount of time, is accomplished. An algorithm for solving this problem by universal variables was used. Then, the optimum maneuver is selected and simulated using the Spacecraft Trajectory Simulator (STRS). In the STRS the orbital movement is obtained by the solution of Kepler's equation for each simulation step. Thus, given an initial state, the Keplerian elements are obtained and propagated to the next step, to be converted into the new state. In the STRS simulator, the reference state is defined by guidance subsystem providing the ideal trajectory to be followed, according to the solution of the TPBVP. This reference is continuously compared with the current position of the vehicle generating an error signal, which is inserted into proportional-integral-derivative controller, generating a signal capable of reducing errors in transition and stationary regimes. This signal is sent to the actuators to generate a signal to be applied in the dynamics model of the movement, added to the disturbing signal due to the gravitational forces of the Sun, Io, Europa, Ganymede and Callisto, and also the second-order term J2 of Jupiter's gravitational potential. Therefore the evolution of the spacecraft's orbit can be simulated and analyzed.

2. Two Point Boundary Value Problem

Determination of the optimal maneuver requires the solution of the Two Point Boundary Value Problem (TPBVP). To solve this problem is necessary to calculate the transfer orbit that connects a point on the initial orbit (initial position of the spacecraft) to another point in the final orbit (final position of the spacecraft), during a given time interval t. The initial and final velocities in the transfer orbit, $\vec{v}_1$ and $\vec{v}_2$, for the initial and final radii vectors, $\vec{r}_1$ and $\vec{r}_2$, and are given by:

$$\vec{v}_1 = \frac{\vec{r}_2 - f(z)\vec{r}_1}{g(z)}; \quad \vec{v}_2 = \frac{\dot{g}(z)\vec{r}_2 - \vec{r}_1}{g(z)} \tag{1}$$

To solve the TPBVP the functions $f(z)$ and $g(z)$ must be found. This problem is known as Gauss's problem or Lambert's problem. A detailed study can be found in Bate et al. (1971). The algorithm for solving this problem through universal variables (Battin, 1999; Bond, 1996; Bate et al., 1971) utilizes the following equations:

$$A = sign(\pi - \Delta\theta)\sqrt{|\vec{r}_1||\vec{r}_2|(1+\cos\Delta\theta)}\,; \qquad \begin{matrix} sign(\pi-\Delta\theta) = -1 \Rightarrow \Delta\theta > \pi \\ sign(\pi-\Delta\theta) = +1 \Rightarrow \Delta\theta < \pi \end{matrix} \tag{2}$$

$$\Delta\theta = a\cos\left(\frac{\vec{r}_1 \cdot \vec{r}_2}{|\vec{r}_1||\vec{r}_2|}\right) \tag{3}$$

$$F(z) = x^3(z)S(z) + A\sqrt{y(z)} - t\sqrt{\mu} = 0 \tag{4}$$

$$S(z) = \frac{\sqrt{z} - \sin(\sqrt{z})}{\sqrt{z^3}}\,; \qquad C(z) = \frac{1-\cos(\sqrt{z})}{z} \tag{5}$$

$$x(z) = \sqrt{\frac{y(z)}{C(z)}}\,; \qquad y(z) = |\vec{r}_1| + |\vec{r}_2| - A\frac{1-zS(z)}{\sqrt{C(z)}} \tag{6}$$

$$\left\{ z \in \Re : 0 \le z \le (2\pi)^2 \right\} \tag{7}$$

The function F(z) is swept by using a cascade algorithm and covers the entire range of elliptical solutions, as described in Battin (1999). The sweep is processed n times, each ruled by the $F(z)$ tolerance and the step size. This approach enables us to obtain a precision solution without the necessity of the initial guess of the variables, since this approach depends only on the variable z which is analyzed for the whole range that represents the elliptical solutions. When the method converges to a solution evaluate the functions $f(z)$ and $g(z)$.

$$f(z) = 1 - \frac{y(z)}{|\vec{r}_1|}\,; \qquad g(z) = A\sqrt{\frac{y(z)}{\mu}}\,; \qquad \dot{g}(z) = 1 - \frac{y(z)}{|\vec{r}_2|} \tag{8}$$

Then, calculate the transfer velocities $\vec{v}_1$ and $\vec{v}_2$. With the velocities in the initial and final orbits, the necessary velocity increments can be obtained.

$$\Delta\vec{v}_1 = \vec{v}_1 - \vec{v}_{initial}\,; \quad \Delta\vec{v}_2 = \vec{v}_{final} - \vec{v}_2 \tag{9}$$

To obtain the optimum impulsive maneuver, which minimizes the fuel consumption minimizing the total velocity increment, the solution of the TPBVP is obtained several times varying the time interval spent in the maneuver. The maneuver with the minimum velocity increment is chosen to be simulated, but now considering a non-impulsive model of the propulsion system.

3. Spacecraft Trajectory Simulator

The Spacecraft Trajectory Simulator (STRS), developed by Rocco (2008), and utilized by Rocco (2009, 2012, 2013) and by Rocco et al. (2010), was used to simulate the orbital trajectory. The STRS uses a closed loop control system for the trajectory. In the simulation, the orbital movement can be obtained by solving the Kepler equation (Eq. 10) for each step of the simulation, where M is the mean anomaly, u is the eccentric anomaly and e is the eccentricity of the orbit.

$$M = u - e\sin u \tag{10}$$

Given an initial state and a time interval, the state (position and velocity) can be converted into keplerian elements solving the inverse problem of satellite positioning. Then, using the Kepler equation those elements are propagated considering the given time interval. The new spacecraft state can be obtained solving the direct problem of positioning, Kuga et al. (2008).

The architecture of the STRS is presented in Fig. 1. The reference trajectory can be obtained from a guidance sub-system capable of providing the optimal path to be followed (solution of the TPBVP). This reference is continuously compared with the current position of the spacecraft. Therefore, an error signal is generated by the difference between the current and reference states. Then, the error signal is sent to a proportional-integral-derivative controller (PID), which the control law is defined by Eq. 11, where K_P is the proportional gain, K_I is the integral gain, K_D is the derivative gain, and $er(t)$ is the error signal.

$$c(t) = K_P\, er(t) + K_I \int er(t)\,\mathrm{d}t + K_D \frac{\mathrm{d}er(t)}{\mathrm{d}t} \tag{11}$$

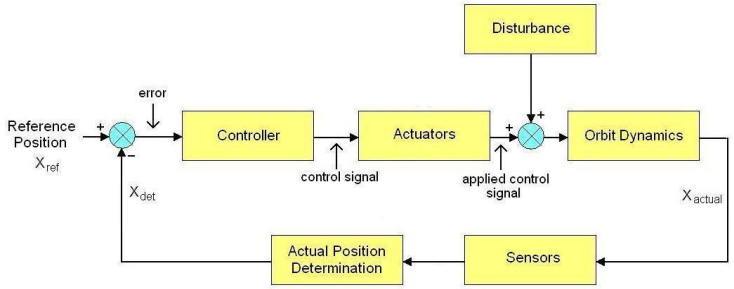

Figure 1. Architecture of the trajectory control system in closed loop

The controller will generate a signal to reduce the error. Then, this signal is sent to the propulsion system. At this time, considering the actuator model, a signal is generated to be applied in the dynamic model. Then the current state of the spacecraft is determined. A sub-system containing the sensor model is used to estimate the current state, considering an inertial coordinate system centered at the center of the Mars. Finally, the current position of the satellite is compared with the reference position, and the cycle starts again.

4. Orbital Disturbance

The evaluation of the errors in the trajectory becomes even more relevant if the effects of orbital perturbations acting on the spacecraft were considered. Thus, deviations in the trajectory due to disturbances caused by the Jupiter gravitational potential (second-order term *J*2) and the gravitational attractions of the Sun, Io, Europa, Ganymede and Callisto were included in the simulations. The mathematical models of these perturbations in the motion of a spacecraft can be found in , Chobotov (1991) and Kaula (1966).

The function of the gravitational potential due to the presence of a third celestial body is given by Eq. 12 (Chobotov, 1991), where: μ' is obtained by the product of the gravitational constant and the mass m' of the third body; r' is the absolute position of the third body related to the center of Jupiter; ψ is the angle between the position vector of the spacecraft related to the

Jupiter ($\vec{r}$) and the position vector of the spacecraft related to the third body ($\vec{r}'$); r is the absolute position related to the Jupiter.

$$F' = \left(\frac{\mu'}{r'}\right)\left[1+\sum_{n=2}^{\infty}\left(\frac{r}{r'}\right)^n P_n \cos\psi\right] \tag{12}$$

According to Prado and Kuga (2001) and Szebehely (1967) the general problem of three bodies provides a simple way to calculate the disturbing accelerations due to the gravitational attraction of the bodies, obtained from the Newton's law of gravitation:

$$\ddot{\vec{r}}_1 = -G\,m_2\frac{\vec{r}_1-\vec{r}_2}{\left|\vec{r}_1-\vec{r}_2\right|^3} + G\,m_3\frac{\vec{r}_3-\vec{r}_1}{\left|\vec{r}_3-\vec{r}_1\right|^3};\ \ddot{\vec{r}}_2 = -G\,m_3\frac{\vec{r}_2-\vec{r}_3}{\left|\vec{r}_2-\vec{r}_3\right|^3} + G\,m_1\frac{\vec{r}_1-\vec{r}_2}{\left|\vec{r}_1-\vec{r}_2\right|^3};\ \ddot{\vec{r}}_3 = -G\,m_1\frac{\vec{r}_3-\vec{r}_1}{\left|\vec{r}_3-\vec{r}_1\right|^3} + G\,m_2\frac{\vec{r}_2-\vec{r}_3}{\left|\vec{r}_2-\vec{r}_3\right|^3} \tag{13}$$

where $\vec{r}_1$, $\vec{r}_2$ and $\vec{r}_3$ are the positions of the bodies, m_1, m_2 and m_3 the masses of the bodies, and G is the gravitational constant. Using Eq. 13 the disturbing effects on the spacecraft's trajectory can be determined. Taking into account a simulation length 50 orbits, the velocity increment due to the disturbing forces are presented in Fig. 2 to Fig. 7. The spacecraft's orbit considered in this simulation is the same that will be considered as initial orbit for the orbital maneuvers presented in section 5: semi-major axis (a) = 500444 km, eccentricity (e) = 0.0451; inclination (i) = 45º; right ascension of the ascending node (Ω) = 45º; argument of the periapsis (ω) = 45°.

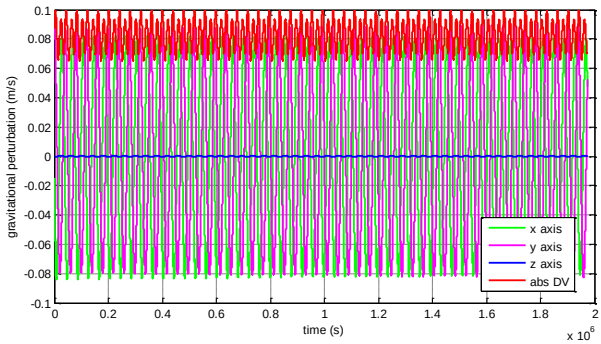

Figure 2. *J*2 disturbing

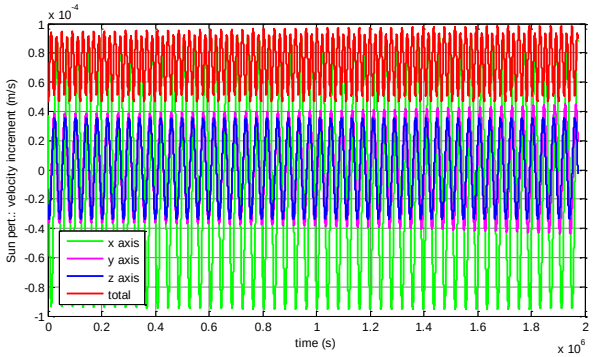

Figure 3. Sun disturbing

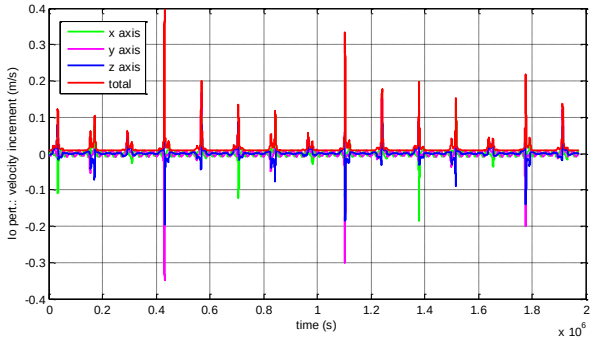

Figure 4. Io disturbing

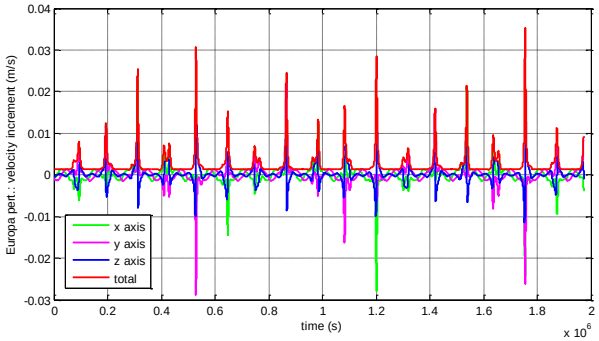

Figure 5. Europa disturbing

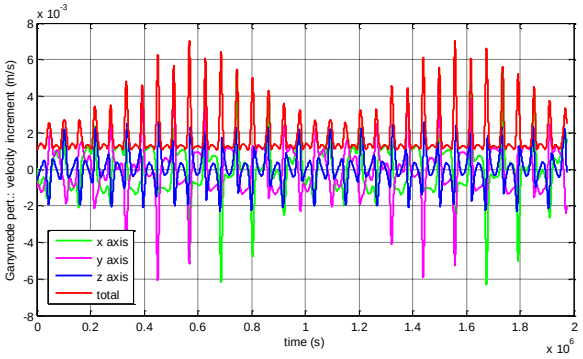

Figure 6. Ganymede disturbing

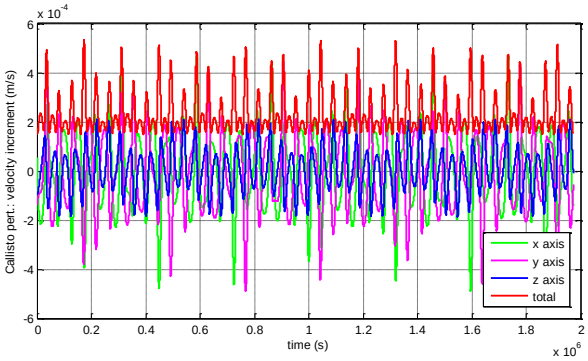

Figure 7. Callisto disturbing

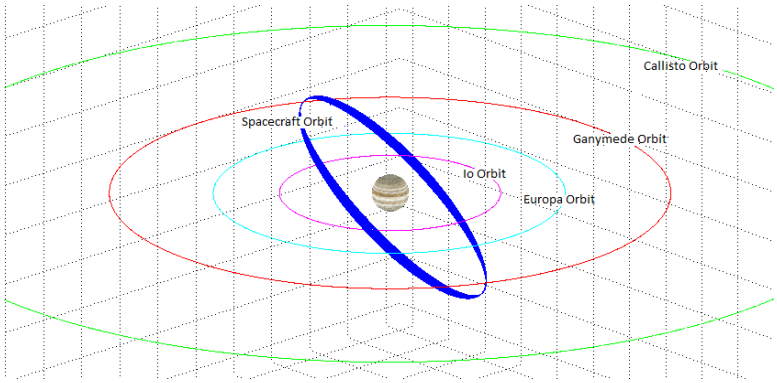

Figure 8. Orbits of the Galilean moons and 50 spacecraft orbits

5. Orbital Maneuver Simulation

Due to the impossibility of application of an infinite thrust the orbital maneuver must be distributed in a propulsive arc around the position of the impulse determined by solution of the TPBVP. In this propulsive arc continuous thrust is applied, limited to the maximum capacity of the thrusters. However, the effect of the propulsive arc is not exactly equivalent to the application of an impulsive thrust. The difference produces a deviation in the final orbit with respect to the reference orbit. The velocity increment applied to the spacecraft, according to Chobotov [6], is given by Eq. 14, where g_0 is the gravitational constant at planet's surface and g at the spacecraft altitude, I_{sp} is the specific impulse, γ is the flight angle formed between the direction of the velocity and the thruster pointing direction, m_i is the mass of the vehicle and m_f the final mass. Therefore, to minimize the error in the final orbit, the flight angle could be maintained near to zero by controlling the pointing direction of the thruster, ensuring that the thrust is always applied in the direction tangential to the path. However, this solution is more complex because it requires the use of the attitude control system, and in fact, this approach is not capable to reduce the error in the final orbit reached by the spacecraft.

$$\Delta V = g_0 I_{sp} \ln \frac{m_i}{m_f} - \int_{t_1}^{t_2} g \sin\gamma \, \mathrm{d}t \tag{14}$$

Hence, to optimize the propulsive maneuvers distributed in an arc it must be considered the optimization procedure for orbital maneuvers with continuous thrust: Edelbanum (1961); Biggs

(1978); Oliveira et al. (2013). However this optimization procedure is a difficult task, since in most of the cases it requires numerical methods and the definition of initial values for obtaining the solution. A simple possibility to minimize the effect caused by the error in the thrust direction would be executing the maneuver in several stages, each one applying just a fraction of the total velocity increment, to reduce each propulsive arc and thereby reduce the flight angle. In this case the error in the trajectory is minimized but the total time spent to reach the final orbit is maximized, characterizing a problem of multi-objective optimization with conflicting objectives. Another possibility to minimize the error in the trajectory after the application of the main thrust could be the use of an automatic correction of the orbital elements using continuous low thrust controlled in closed loop. In this approach, the final orbital elements are defined, then control loops for each of these elements determine, at each step of the simulation, the magnitudes and directions of application of thrust necessary to reach the desired orbital elements. The variations of elements occur gradually until the difference between the current and reference signals do not generate errors. Then, the propulsion system is turned off.

To exemplify the necessity of split the maneuver in several propulsive arcs, or use the automatic correction approach, eight cases were studied: case 1 for impulsive approach; cases 2 to 8 for maneuvers using thruster with capacity of 50 N to 350 N, shown in Figs. 10 to 37, without automatic correction (subcases *a*) and with automatic correction (subcases *b*). The initial orbit is defined by the following keplerian elements: a = 500444 km, e = 0.0451; i = 45º; Ω = 45º; ω = 45°. The final orbit is defined by: a = 536190 km, e = 0.0451; i = 45º; Ω = 45º; ω = 45º. The time necessary to perform the transfer maneuver and the velocity increment applied to the spacecraft for the impulsive approach were determined by the solution of the Lambert's problem (TPBVP): t = 103820 s; Δv_1 = 538.2384 m/s ($\Delta\vec{v}_1 = -230.940508\hat{i} - 35.573704\hat{j} + 138.145192\hat{k}$); Δv_2 = 266.7921 m/s ($\Delta\vec{v}_2 = 227.670409\hat{i} + 38.775178\hat{j} - 133.569099\hat{k}$). In this section was considered a simulation length of 129600 s and a simulation step of 3s.

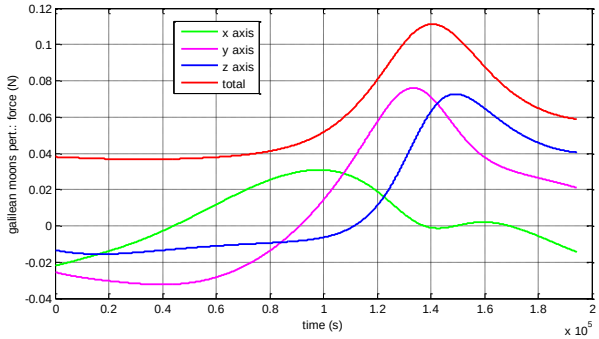

Figure 9. Io disturbing during the maneuver

The error in the semi-major axis and the applied velocity increment for all cases are summarized in Table 1. When considered the application of the impulses, in case 1, all the velocity increment and all change in the semi-major axis are performed instantly. Therefore the applied thrust is in fact a pulse. However, was applied continuous thrust to counteract the disturbances. This continuous thrust was applied because the STRS was adjusted to control the trajectory, reducing the effect produced by the disturbances, but the main orbital maneuver in case 1 (impulsive approach) was performed in an impulsive way.

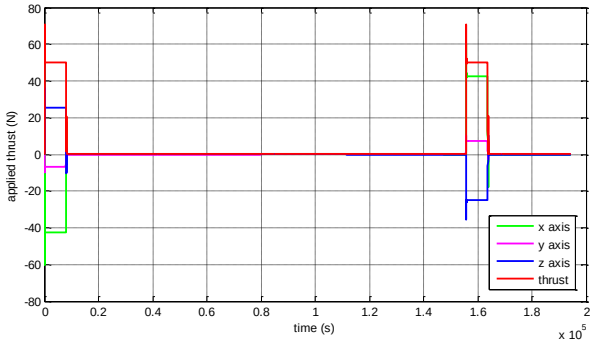

Figure 10. Case 2*a*: thrust (50 N)

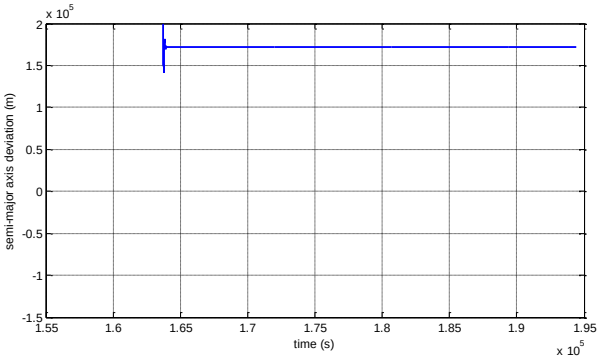

Figure 11. Case 2*a*: semi-major axis error

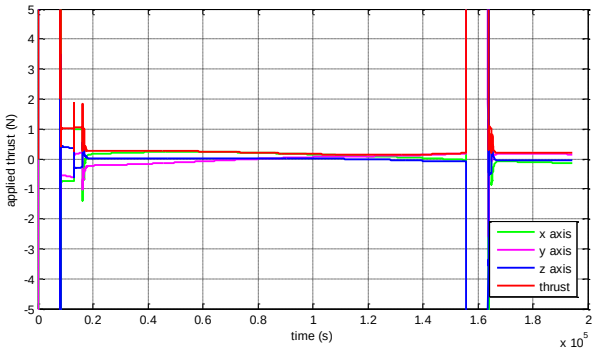

Figure 12. Case 2*b*: thrust (50 N) close-up

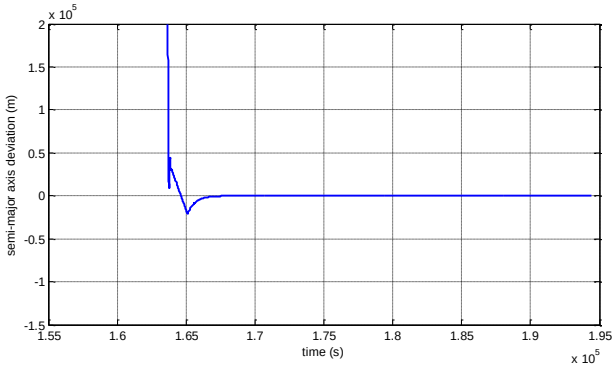

Figure 13. Case 2*b*: semi-major axis error

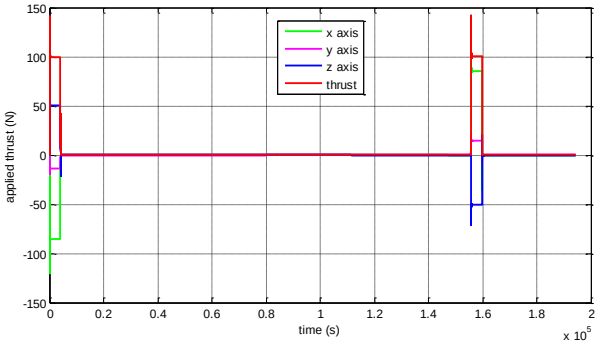

Figure 14. Case 3*a*: thrust (100 N)

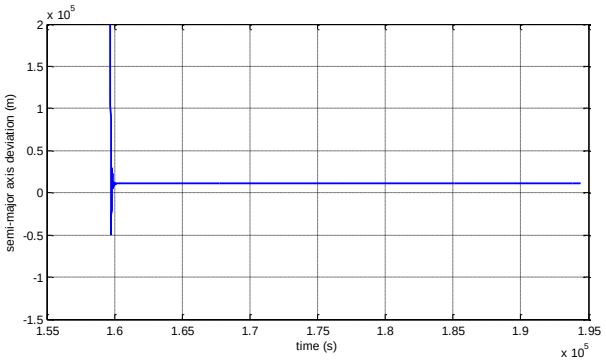

Figure 15. Case 3*a*: semi-major axis error

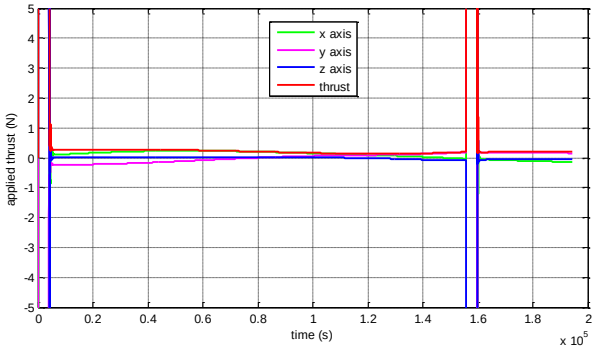

Figure 16. Case 3*b*: thrust (100 N) close-up

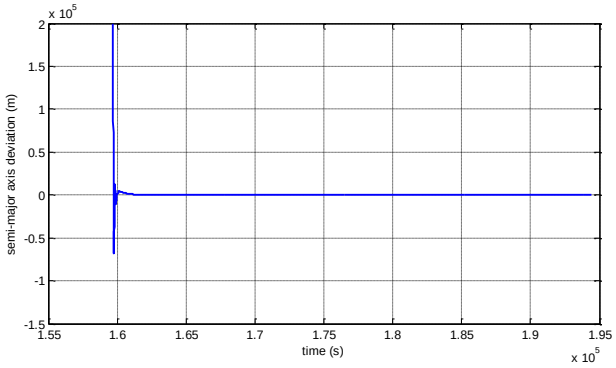

Figure 17. Case 3*b*: semi-major axis error

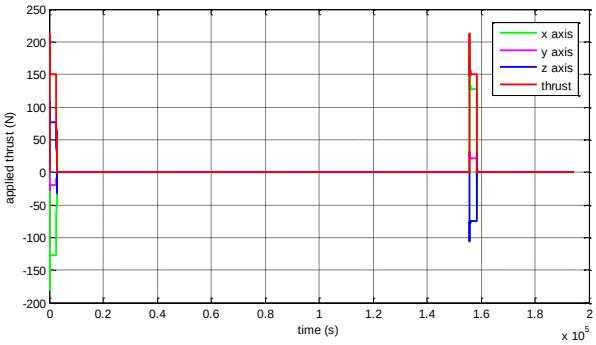

Figure 18. Case 4*a*: thrust (150 N)

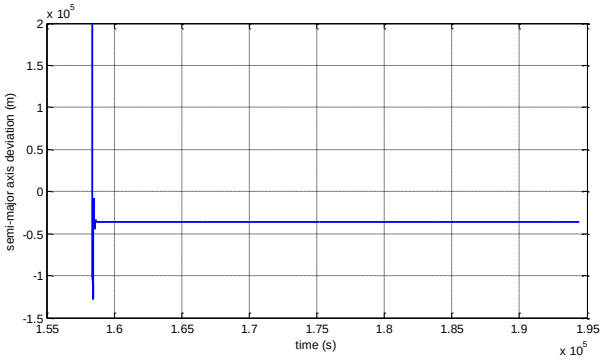

Figure 19. Case 4*a*: semi-major axis error

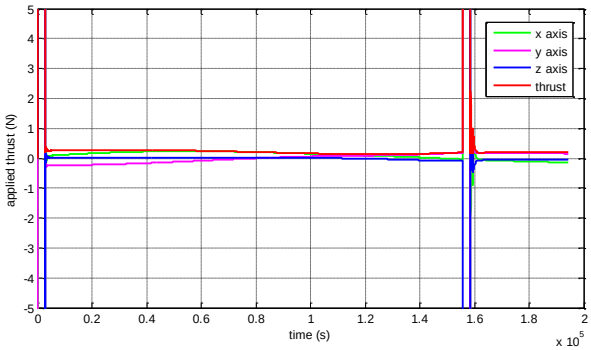

Figure 20. Case 4*b*: thrust (150 N) close-up

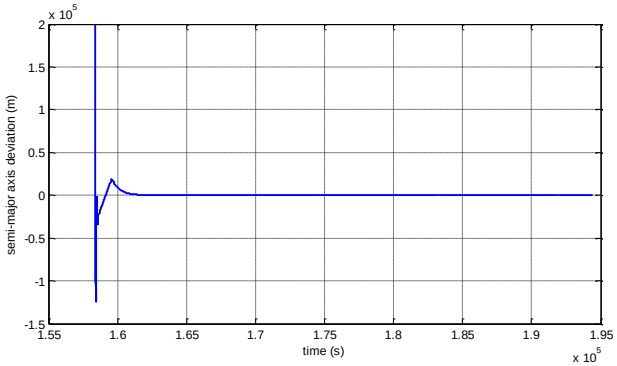

Figure 21. Case 4*b*: semi-major axis error.

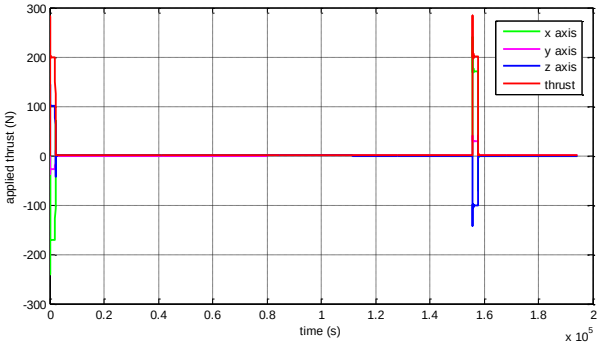

Figure 22. Case 5*a*: thrust (200 N)

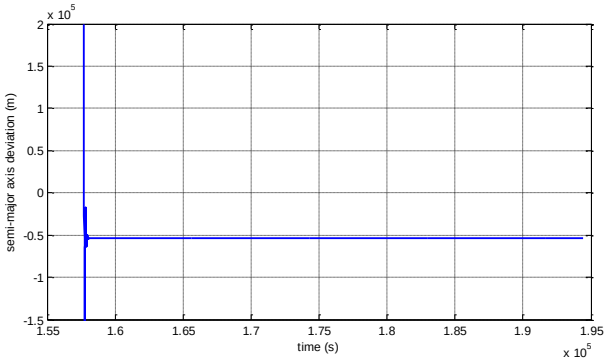

Figure 23. Case 5*a*: semi-major axis error

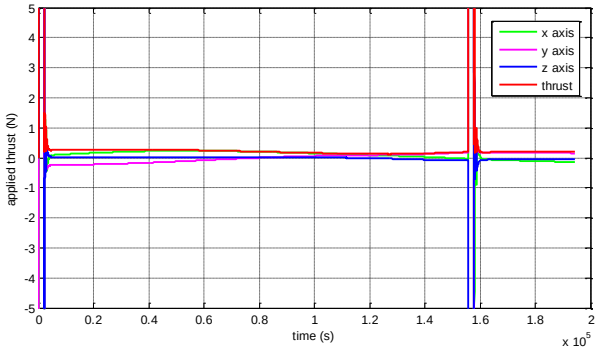

Figure 24. Case 5*b*: thrust (200 N) close-up

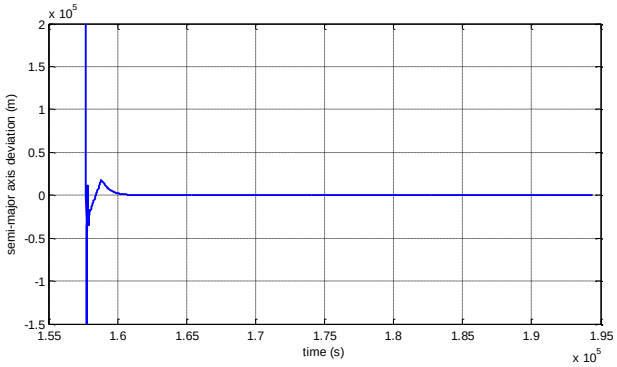

Figure 25. Case 5*b*: semi-major axis error

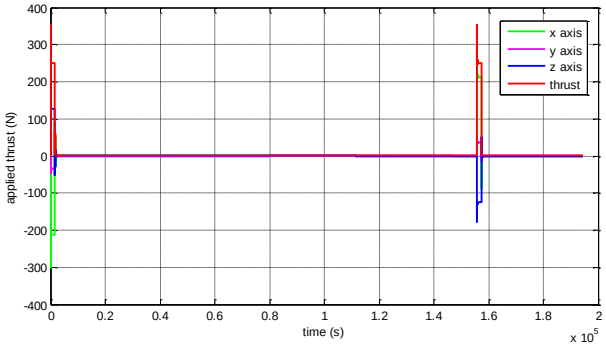

Figure 26. Case 6*a*: thrust (250 N)

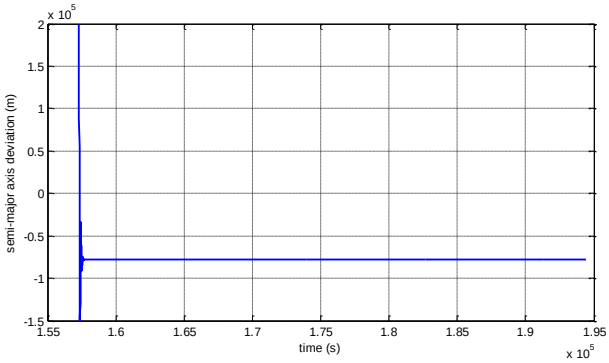

Figure 27. Case 6*a*: semi-major axis error

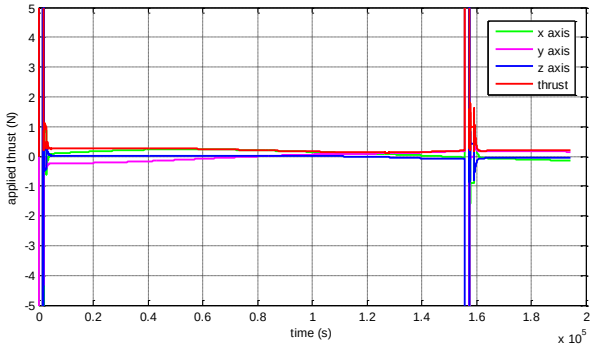

Figure 28. Case 6*b*: thrust (250 N) close-up

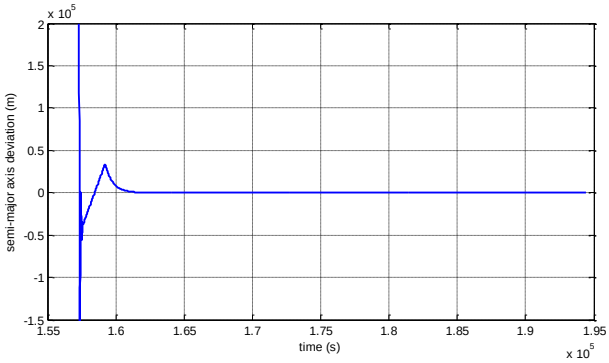

Figure 29. Case 6*b*: semi-major axis error

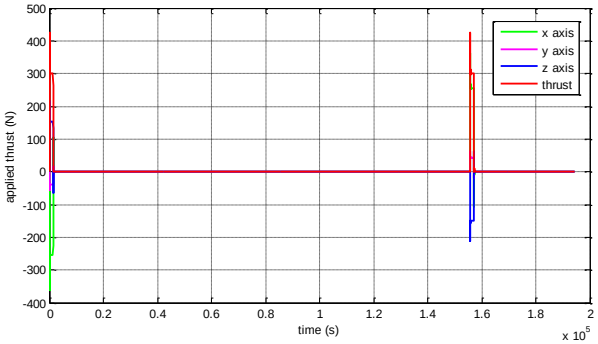

Figure 30. Case 7*a*: thrust (300 N)

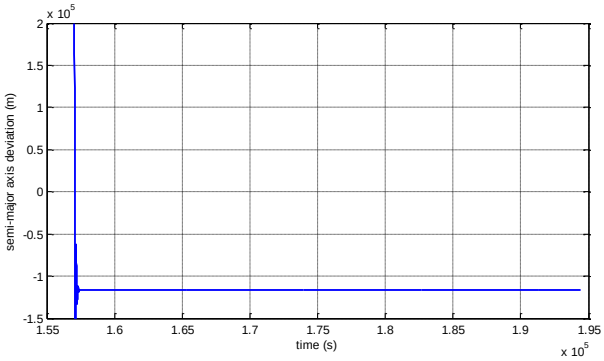

Figure 31. Case 7*a*: semi-major axis error

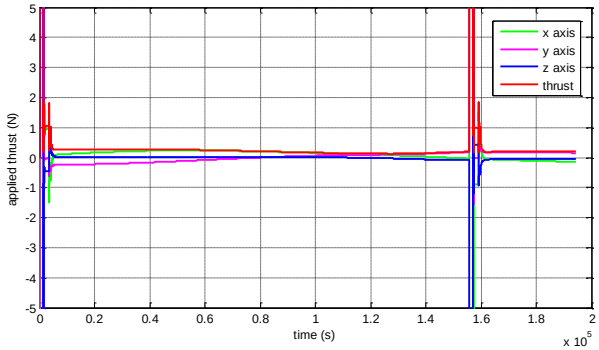

Figure 32. Case 7*b*: thrust (300 N) close-up

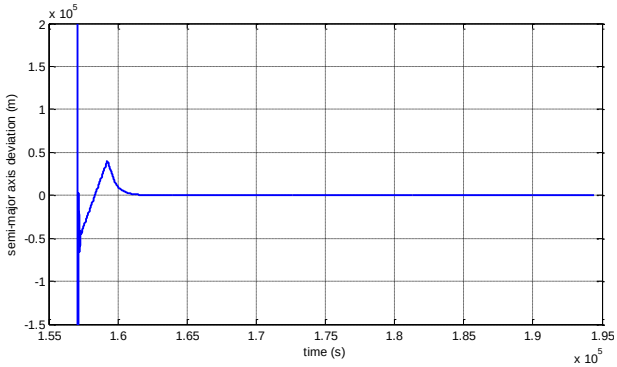

Figure 33. Case 7*b*: semi-major axis error

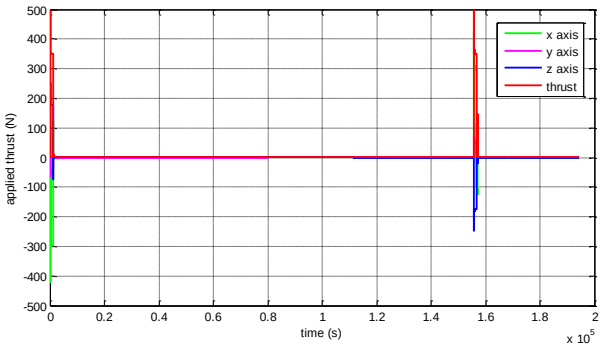

Figure 34. Case 8*a*: thrust (350 N)

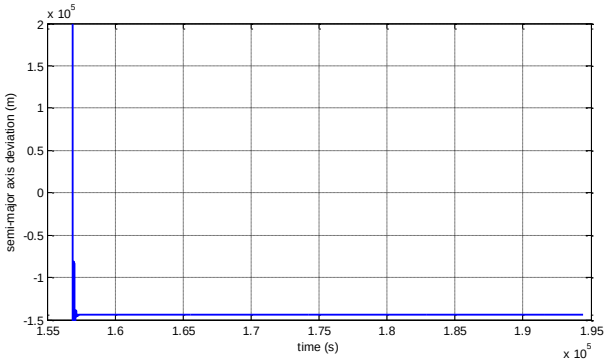

Figure 35. Case 8*a*: semi-major axis error

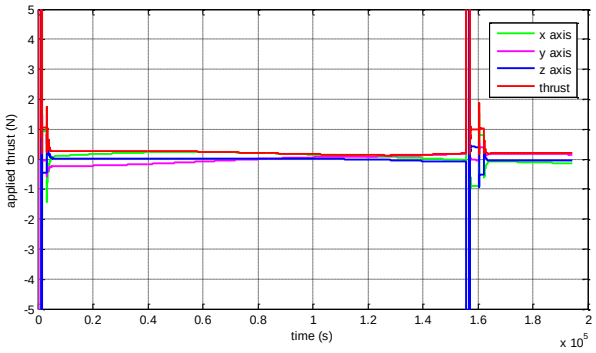

Figure 36. Case 8*b*: thrust (350 N) close-up

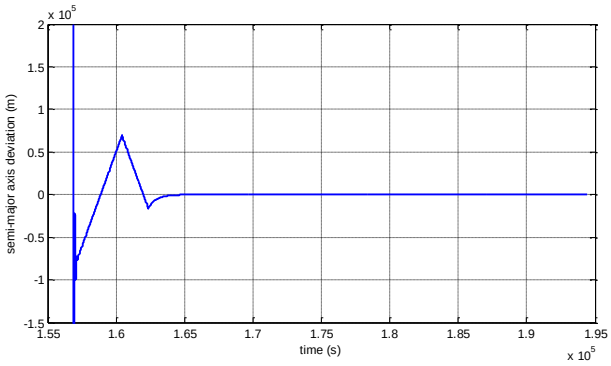

Figure 37. Case 8*b*: semi-major axis error

Table 1. Semi-major axis error and total applied velocity increment

Thrust Capacity	Semi-Major Axis Error (km)		Total Applied Velocity Increment (m/s)	
	without automatic correction subcase *a*	with automatic correction subcase *b*	without automatic correction subcase *a*	with automatic correction subcase *b*
Case 2: 50 N	172.31398380	**0.00019550**	565.42102984	570.55202300
Case 3: 100 N	10.90866292	**0.00000848**	569.53735895	569.87503114
Case 4: 150 N	35.91877973	**0.00000522**	572.80670438	573.58799460
Case 5: 200 N	53.58403656	**0.00000696**	575.67561016	576.79717998
Case 6: 250 N	78.21009687	**0.00000928**	578.67061316	580.50302756
Case 7: 300 N	116.75456302	**0.00001878**	581.82111301	584.73286753
Case 8: 350 N	144.38659081	**0.00000039**	584.85888182	589.14904132

In general the results present a bigger error for the semi-major axis, for the subcase *a*, compared with the impulsive approach. However, using the automatic correction, the error was continually reduced to almost zero after the application of the main thrust. Thus, in a mission analysis of a spacecraft should be considered all possible combinations of the main thrust and the automatic correction, to choose the best solution. In this study the performance of the automatic correction was excellent and was able to correct the errors generated by the fact that the main thrust was distributed in a propulsive arc instead of an impulse. With this new procedure was possible to eliminate almost all deviations related to the reference trajectory for all cases studied.

3. Conclusions

This work represents an effort in the design of the propulsion system of space vehicles. It was confirmed that the effect of a propulsive arc is not exactly equivalent to the application of an impulse. The difference produces a deviation of the final orbit relative to the reference orbit. This deviation depends on the magnitude of the impulse required for the maneuver, the maximum capacity of the propulsion system and the characteristics of the trajectory control system, as seen in the results. Thus, the evaluation of the trajectory deviations is relevant to the analysis of a space mission and in the design of the trajectory control system if a more realistic model is considered instead of the ideal case represented by the impulsive approach.

7. References

[1] Bate, R.R., Mueller, D.D., White, J.E. "Fundamentals of Astrodynamics." Dover Publications, New York, 1971.

[2] Battin, R. H. "An Introduction to the Mathematics and Methods of astrodynamics, Rev. ed." AIAA Educational Series, Reston, 1999.

[3] Biggs, M.C.B. "The Optimization of Spacecraft Orbital Manoeuvres. Part I: Linearly Varying Thrust Angles." The Hatfield Polytechnic, Numerical Optimization Centre, 1978.

[4] Bond, V. R., Allman, M. C. "Modern Astrodynamics: fundamentals and perturbation methods." Princeton University Press, New Jersey, 1996.

[5] Chobotov, V.A. "Orbital Mechanics." Washington, DC: American Institute of Aeronautics and Astronautics, Inc., 365p., 1991.

[6] Edelbanum, T.N. "Propulsion Requirements for Controllable Satellites." ARSJ, 1961.

[7] Kaula, W.M. "Theory of Satellite Geodesy Applications of Satellites to Geodesyc." Blaisdell Pub. Co., 1966.

[8] Kuga, H.K., Rao, K.R., Carrara, V. "Introdução à Mecânica Orbital." Instituto Nacional de Pesquisas Espaciais, INPE-5615-PUD/064, São José dos Campos, 2008.

[9] Oliveira, T.C., Rocco, E.M., Ferreira, J.L., Prado, A.F.B.A. "Minimum Fuel Low-Thrust Transfers for Satellites Using a Permanent Magnet Hall Thruster." Mathematical Problems in Engineering, v. 2013, pp. 1-12, 2013.

[10] Prado, A.F.B.A, Kuga, H.K. (Eds.) "Fundamentos de Tecnologia Espacial." Instituto Nacional de Pesquisas Espaciais, São José dos Campos, 2001. ISBN: 85-17-00004-8

[11] Rocco, E. M. "Perturbed orbital motion with a PID control system for the trajectory." In: Colóquio Brasileiro de Dinâmica Orbital-CBDO2008, Águas de Lindóia, 2008.

[12] Rocco, E.M. "Earth Albedo Model Evaluation and Analysis of the Trajectory Deviation for some Drag-Free Missions." Proceedings of the 8th Brazilian Conference on Dynamics Control and Applications-DINCON'09, Bauru, May 18-22, 2009.

[13] Rocco, E.M. "Controle de trajetória com propulsão continua para missões do tipo drag-free." In: Congresso Nacional de Engenharia Mecânica-CONEM2012, São Luís, 2012.

[14] Rocco, E.M. "Automatic correction of orbital elements using continuous thrust controlled in closed loop." Proceedings CBDO 2012, Journal of Physics: Conference Series, vol. 465, 2013.

[15] Rocco, E. M., Marcelino, E.W., Prado, A.F.B.A. "Closed Loop Control System Applied to Transfer Maneuvers Using Continuous Thrust." Mathematical Problems in Engineering, Aerospace and Sciences, S. J. Campos, 2010.

[16] Rocco, E. M., Souza, M. L. O., Prado, A. B. A. "Station Keeping of Constellations Using Multiobjective Strategies. Mathematical Problems in Engineering, vol. 2013, doi:10.1155/2013/476451

[17] Szebehely, V. Theory of orbits. Academic Press Inc. New York, 1967.